Generalized chaos expansion of state space models for uncertainty quantification in thermoacoustics

By C. F. Silva†, P. Pettersson‡, G. Iaccarino AND M. Ihme

The present study combines intrusive generalized Chaos Expansion (gCE) with a state space thermoacoustic model to account for uncertainty. The acoustic waves, flame response and acoustic reflection coefficients are modeled as stochastic variables and projected onto a finite set of basis functions. By solving the resulting set of equations once, it is possible to determine probability density functions of acoustic quantities at each node of the discretized domain. Two different problems are studied: combustion noise and combustion instability of a typical turbulent swirled combustor. Results of the proposed method are satisfactorily validated against Monte Carlo simulation. The present work is a first step towards the application of the gCE theory in the field of combustion dynamics and thermoacoustics.

1. Introduction

Modern gas turbine designs require operation in lean combustion regimes. Implementation of such designs is, however, impeded by the unpredictable and recurrent appearance of combustion instabilities (Lieuwen & Yang 2005). These instabilities cause strong oscillations of the physical variables (velocity, pressure, temperature, etc.) that characterize the gas turbine, which in turn lead to malfunctioning or destruction of the system. Modern gas turbines designs also aim at reducing combustion noise.

Combustion instabilities and combustion noise are caused by phenomena that are extremely sensitive to any change in the operating condition. Uncertainty Quantification (UQ) of such phenomena is, therefore, crucial in order to design reliable combustors with safety margins. When UQ is applied in thermoacoustics, a strategy in two steps is frequently followed:

(*a*) Simplification of the equations: In order to decrease the computational cost, Reduced Order Models (ROMs) are derived from the reacting Navier-Stokes equations. This is done by making assumptions and simplifications such as linearization around an operating condition. Furthermore, surrogate models can be obtained from ROMs by additional assumptions such as small variance of the input random variables (Bauerheim *et al.* 2014; Magri *et al.* 2016; Silva *et al.* 2017*a*).

(*b*) Sampling of the probability space: In order to collect sufficient statistical data, multiple computations must be performed on the ROM or surrogate model. Except for the work of Avdonin *et al.* (2018) and Mensah *et al.* (2018), the Monte Carlo method has until now been the only one used in combustion dynamics (Bauerheim *et al.* 2014; Magri *et al.* 2016; Silva *et al.* 2017*a*), because it is easy to implement and because it provides

† Technische Universität München, Germany
‡ Norwegian Research Center NORCE, Norway

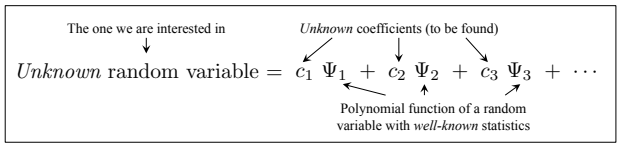

FIGURE 1. Representation of a random variable.

reliable results as long as a significant amount of data (more than tens of thousands samples) can be retrieved.

The aforementioned strategy leads to a dead-end in UQ based on complex models, where a single computation is expensive. To overcome this deficiency we need a change of paradigm.

1.1. *Generalized Chaos expansion*

For a general class of random variables $\boldsymbol{\xi} = (\xi_1, \ldots, \xi_d)$ with zero means and unit variances, any finite-variance function of $\boldsymbol{\xi}$ can be described as a weighted sum of orthogonal stochastic basis functions $\{\Psi_i\}_{i=1}^{\infty}$, as illustrated in Figure 1. The set $\{\Psi_i\}_{i=1}^{\infty}$ is a basis of the L^2 space weighted by the Probability Density Functions (PDF) of $\boldsymbol{\xi}$. The coefficients $\{c_i\}_{i=1}^{\infty}$ may be functions of space and time, admitting a separation of stochastic and physical space. The stochastic Galerkin method can be used to obtain the expansion coefficients that characterize the output random variables when the input random variables are Gaussian (Ghanem & Spanos 1991). For treatment of stochastic processes that are not Gaussian, Xiu & Karniadakis (2002) introduced a generalized Chaos Expansion (gCE), where the basis functions of the series could be of any type of hypergeometrical polynomials of the Askey scheme.

Two variants of solution methods are encountered in gCE approaches to compute the stochastic modes: non-intrusive gCE and intrusive gCE. In the former method, several deterministic computations are performed in order to create a collection of realizations of the output of interest. Afterwards, quadrature rules are applied to approximate the coefficients of each polynomial. In thermoacoustics, this method has been applied in the work of Avdonin *et al.* (2018). In the igCE method, each stochastic variable is expanded in polynomial series and the system of equations is projected onto the space spanned by the basis functions. Subsequently, the resulting enlarged and modified system of equations is solved once in order to find the coefficients of each polynomial. Significant theoretical progress on gCE has been achieved during the past decade in the field of applied mathematics (Le Maître & Knio 2010; Bijl *et al.* 2013; Najm 2009).

2. The state space model

A generic state space model reads

$$\dot{\boldsymbol{x}} = \tilde{A}\boldsymbol{x} + \tilde{B}\tilde{\boldsymbol{u}}, \tag{2.1}$$

$$\boldsymbol{y} = \tilde{C}\boldsymbol{x} + \tilde{D}\tilde{\boldsymbol{u}}, \tag{2.2}$$

$$\tilde{\boldsymbol{u}} = F\boldsymbol{y} + \boldsymbol{u}, \tag{2.3}$$

where the vectors $\boldsymbol{x}$, $\boldsymbol{u}$ and $\boldsymbol{y}$ stand for the system states, inputs and outputs, respectively. Additionally, the state matrix $\tilde{A}$ characterizes the system states, the input matrix $\tilde{B}$ connect the inputs to the states, the output matrix $\tilde{C}$ relates the outputs to the states,

the feedthrough matrix $\tilde{D}$ directly relates inputs to outputs, and the connectivity matrix F connects all subsystems in a single system. Finally, Eqs. (2.2) and (2.3) are combined to obtain $\tilde{\boldsymbol{u}}(I - F\tilde{D}) = F\tilde{C}\boldsymbol{x} + \boldsymbol{u}$, and introduced in Eq. (2.1) to obtain

$$\dot{\boldsymbol{x}} = \underbrace{\left(\tilde{A} + \tilde{B}(I - F\tilde{D})^{-1}F\tilde{C}\right)}_{A}\boldsymbol{x} + \underbrace{B(I - \tilde{F}D)^{-1}\boldsymbol{u}}_{-\boldsymbol{b}}. \tag{2.4}$$

By applying the Laplace transform to Eq. (2.4), written as $\mathcal{L}\{a(t)\} = \hat{a}$, we obtain the frequency description of the system under investigation

$$A\hat{\boldsymbol{x}} - s\hat{\boldsymbol{x}} = \hat{\boldsymbol{b}}, \tag{2.5}$$

where $\mathcal{L}\{\dot{\boldsymbol{x}}(t)\} = s\hat{\boldsymbol{x}}$, and $s = \sigma + \boldsymbol{i}\omega$ is the Laplace variable, whose real part σ denotes the growth rate, and the imaginary part represents the oscillation frequency of the thermoacoustic mode $\hat{\boldsymbol{x}}$. Equation (2.5) is a linear system and describes the acoustic scattering and combustion noise for different frequencies ω while imposing $\sigma = 0$. Additionally, the corresponding eigenvalue problem reads

$$A\hat{\boldsymbol{x}} = \mu\hat{\boldsymbol{x}}, \tag{2.6}$$

which is used to study the thermoacoustic stability of the system. The eigenvectors $\hat{\boldsymbol{x}}$ characterize the thermoacoustic modes, and the eigenvalue μ characterizes the growth rate σ and resonant frequency ω of each thermoacoustic mode. A stable system implies a negative growth rate $\sigma < 0$. Contrary to the homogeneous Helmholtz equation, which has been used in many combustion instability studies (Nicoud *et al.* 2007) and defines a nonlinear eigenvalue problem, the resulting system in Eq. (2.6) defines a linear eigenvalue problem, even for cases that account for non-ideal boundary conditions and non-negligible flame dynamics. In the following, the symbol $\hat{[\,]}$ is dropped for readability purposes.

3. The stochastic state space (SSS) model

The formulation of the SSS model depends on the type of UQ problem to be solved. If UQ of the scattering acoustic behavior or the noise produced by combustion is of interest, an extended linear system of equations is solved (Section 3.1). If, on the contrary, thermoacoustic stability needs to be investigated, one solves a single multi-parameter eigenvalue problem (Section 3.2).

3.1. *Extended linear system*

In this work we consider uncertainties in the acoustic reflection at the boundaries and in the delay of the flame response model. This implies that the matrices $\tilde{A}$, $\tilde{B}$ and $\tilde{F}$ are stochastic. Accordingly, the elements in Eq. (2.4) are expanded as a gCE series truncated to a finite number of terms P,

$$\boldsymbol{x} = \sum_{l=1}^{P}\Psi_l\boldsymbol{x}_l, \quad \boldsymbol{u} = \sum_{l=1}^{P}\Psi_l\boldsymbol{u}_l, \quad \boldsymbol{y} = \sum_{l=1}^{P}\Psi_l\boldsymbol{y}_l, \quad K = \sum_{l=1}^{P}\Psi_l K_l, \tag{3.1}$$

where K denotes either matrix $\tilde{A}$, $\tilde{B}$ or F. Note that the gCE coefficients can be scalars, vectors or matrices. In the following example, it is shown how a stochastic system of equations is built from a generic model.

Example 1

We consider an algebraic equation $ax = b$, where b and a are known stochastic input parameters that can be expanded similarly to the expressions in Eq. (3.1). The solution of this equation reads $x = b/a$ if $a \neq 0$. The algebraic model $\sum_l \sum_k \Psi_l \Psi_k a_l x_k = \sum_l \Psi_l b_l$ is projected on the set of basis functions Ψ_j where $j = 1, \cdots, P$ to obtain

$$\mathbb{E}\left(\Psi_j \sum_{k=1}^{P}\sum_{l=1}^{P} \Psi_k \Psi_l a_k x_l\right) = \mathbb{E}\left(\Psi_j \sum_{l=1}^{P} \Psi_l b_l\right) \Rightarrow \quad \sum_{k=1}^{P}\sum_{l=1}^{P} \mathbb{E}\left(\Psi_j \Psi_k \Psi_l\right) a_k x_l = b_j, \tag{3.2}$$

where $\mathbb{E}(\cdot)$ denotes the expectation operator with respect to the random variables. The P system of equations can be written as

$$\underbrace{\begin{bmatrix} G^{\mathrm{SG}}(\boldsymbol{a})_{1,1} & \cdots & G^{\mathrm{SG}}(\boldsymbol{a})_{1,P} \\ \vdots & & \vdots \\ G^{\mathrm{SG}}(\boldsymbol{a})_{P,1} & \cdots & G^{\mathrm{SG}}(\boldsymbol{a})_{P,P} \end{bmatrix}}_{\mathbf{G}(\boldsymbol{a})} \underbrace{\begin{bmatrix} x_1 \\ \vdots \\ x_P \end{bmatrix}}_{\boldsymbol{x}} = \underbrace{\begin{bmatrix} b_1 \\ \vdots \\ b_P \end{bmatrix}}_{\boldsymbol{b}}, \tag{3.3}$$

where the stochastic Galerkin matrix

$$G^{\mathrm{SG}}(\boldsymbol{a})_{j,k} = \sum_{l=1}^{P} a_l \mathbb{E}\left(\Psi_j \Psi_k \Psi_l\right) \quad j = 1, \ldots, M, \quad k = 1, \ldots, P, \tag{3.4}$$

has been introduced. Finally, the system of equations is solved for the P unknowns x_j.

Following the same procedure as in Example 1, we obtain the stochastic Galerkin projection of Eq. (2.4),

$$\underbrace{\begin{bmatrix} M_{1,1} & \cdots & M_{1,P} \\ \vdots & & \vdots \\ M_{P,1} & \cdots & M_{P,P} \end{bmatrix}}_{\mathbf{M}} \underbrace{\begin{bmatrix} \boldsymbol{x}_1 \\ \vdots \\ \boldsymbol{x}_P \end{bmatrix}}_{\boldsymbol{x}} = \underbrace{\begin{bmatrix} \boldsymbol{b}_1 \\ \vdots \\ \boldsymbol{b}_P \end{bmatrix}}_{\boldsymbol{b}} \tag{3.5}$$

where

$$M_{j,k} = G^{\mathrm{SG}}(\tilde{\mathbf{A}})_{j,k} + T\tilde{C}\ H^{\mathrm{SG}}(\tilde{\mathbf{B}}, \tilde{\mathbf{F}})_{j,k} - s\delta_{jk}, \quad \boldsymbol{b}_n = \tilde{B}_n T \boldsymbol{u}, \quad T = (I - F_0 D)^{-1} \tag{3.6}$$

and

$$H^{\mathrm{SG}}(\boldsymbol{v}, \boldsymbol{w})_{j,k} = \sum_{l=1}^{P}\sum_{m=1}^{P} v_l w_m \mathbb{E}\left(\Psi_j \Psi_k \Psi_l \Psi_m\right). \tag{3.7}$$

Note that the gCE coefficients are not stochastic, and therefore uncertainty quantification of the system can be performed without sampling. We highlight also that the resulting SSS system (Eq. (3.5)) is linear. Nevertheless, the propagation of input uncertainties to the output random variable $\boldsymbol{x}$ is nonlinear because (a) the inverse problem $\boldsymbol{x} = \mathbf{M}^{-1}\boldsymbol{b}$ is nonlinear; (b) the matrices $M_{j,k}$ are nonlinear in some input parameters, e.g., the time delay τ; (c) the matrix T is nonlinear in the matrices F_0 and D.

3.2. *Multi-parameter eigenvalue problem*

The eigenvalue problem given by Eq. (2.6) with the truncated expansions of Eq. (3.1) is projected onto the space of the first M basis functions, where M is to be determined. The result is the extended system

$$\underbrace{\begin{bmatrix} G^{\mathrm{SG}}(\boldsymbol{a}_{11}) & \dots & G^{\mathrm{SG}}(\boldsymbol{a}_{1n}) \\ \vdots & & \vdots \\ G^{\mathrm{SG}}(\boldsymbol{a}_{n1}) & \dots & G^{\mathrm{SG}}(\boldsymbol{a}_{nn}) \end{bmatrix}}_{\mathbf{B}_0} \boldsymbol{x} - \begin{bmatrix} G^{\mathrm{SG}}(\boldsymbol{\mu}) & & \\ & \ddots & \\ & & G^{\mathrm{SG}}(\boldsymbol{\mu}) \end{bmatrix} \boldsymbol{x} = \mathbf{0}, \tag{3.8}$$

where $\boldsymbol{a}_{ij} = (a_{ij,1}, \dots, a_{ij,P})^T$ $(i, j = 1, \dots, n)$ is the vector of gCE coefficients of the (i, j) entry of A in Eq. (2.6). For $i = 1, \dots, P$, let $\mathbf{B}_i$ be block-diagonal matrices where diagonal block j is the $M \times P$ matrix $[B_i^j]_{k,l} = \mathbb{E}(\Psi_i \Psi_k \Psi_l)$. Equation (3.8) is a Multi-parameter Eigenvalue Problem (MEP), i.e., a generalization of a standard eigenvalue problem of the form

$$\mathbf{B}_0 \boldsymbol{x} + \sum_{i=1}^{P} \lambda_i \mathbf{B}_i \boldsymbol{x} = \mathbf{0}, \tag{3.9}$$

following the single-equation formulation in Browne & Sleeman (1982). Here, the matrix $\mathbf{B}_0$ is derived from the non-symmetric matrix A in Eq. (2.6), so both the multi-parameter eigenvalues λ_i and their corresponding eigenvectors are expected to be complex. The multi-eigenvalues λ_i here correspond to the gCE of the complex eigenvalues μ. Often, $M = P$, but this is not always a suitable choice, as the following example demonstrates.

Example 2

Consider the simplified scalar eigenvalue problem

$$a(\xi)x(\xi) - \lambda(\xi)x(\xi) = 0,$$

where the eigenvalue solution is clearly $\lambda(\xi) = a(\xi)$. Assuming a random variable ξ with unit variance and even PDF, we perform Galerkin projection with $M = P = 2$,

$$\begin{bmatrix} a_1 & a_2 \\ a_2 & a_1 \end{bmatrix} \begin{bmatrix} x_1 \\ x_2 \end{bmatrix} - \begin{bmatrix} \lambda_1 & \lambda_2 \\ \lambda_2 & \lambda_1 \end{bmatrix} \begin{bmatrix} x_1 \\ x_2 \end{bmatrix} = \begin{bmatrix} 0 \\ 0 \end{bmatrix}.$$

Any λ satisfying $\lambda_1 + \lambda_2 = a_1 + a_2$ is a solution with a non-trivial eigenvector (x_1, x_2). In general, a unique solution $\lambda = a$ requires $M > P$. The rationale is that the product of two P-term chaos expansions is in a space of higher-order expansions, e.g., the first $2P - 1$ polynomial basis functions in the case of classical orthogonal polynomials.

3.2.1. *Diagonalizable multi-parameter eigenvalue problems*

As demonstrated in Example 2 above, the multi-parameter eigenvalue problem of Eq. (3.9) is in general under-determined for the square matrix case $M = P$. However, if the stochastic Galerkin matrix of Eq. (3.4) has an eigenvalue decomposition with eigenvectors that are independent of the argument $\boldsymbol{v}$, the $nP \times nP$ MEP becomes a set of P decoupled standard eigenvalue problems, and thus a unique solution exists. Stochastic basis functions that admit diagonalization include zeroth and first-order multiwavelets, as demonstrated in (Pettersson *et al.* 2014). For these cases of special basis functions, we will devise a strategy to find the solution of the MEP.

PROPOSITION 1. *Assume that $G^{\mathrm{SG}}(\cdot) \in \mathbb{C}^{P \times P}$ can be diagonalized with constant eigenvectors, i.e.,*

$$G^{\mathrm{SG}}(\boldsymbol{v}) = Q\Lambda(\boldsymbol{v})Q^T, \quad \forall \boldsymbol{v} \in \mathbb{C}^P.$$

Then the solution of the associated MEP (3.9) *can be obtained by solving P independent standard eigenvalue problems, each of size $n \times n$ with n being the number of degrees of freedom of the deterministic eigenvalue problem.*

The following proof is constructive in the sense that it devises a method to obtain the MEP solution.

Proof. Left-multiplying Eq. (3.8) by $Q^T \otimes I_n$, and setting $\boldsymbol{y} = (Q^T \otimes I_n)\boldsymbol{x}$, yields

$$\begin{bmatrix} \Lambda(\boldsymbol{\mu}) & & \\ & \ddots & \\ & & \Lambda(\boldsymbol{\mu}) \end{bmatrix} \boldsymbol{y} - \begin{bmatrix} \Lambda(\boldsymbol{a}_{11}) & \dots & \Lambda(\boldsymbol{a}_{1n}) \\ \vdots & & \vdots \\ \Lambda(\boldsymbol{a}_{n1}) & \dots & \Lambda(\boldsymbol{a}_{nn}) \end{bmatrix} \boldsymbol{y} = \boldsymbol{0}. \tag{3.10}$$

Let E be the $(nP \times nP)$ permutation matrix with $(n \times P)$ submatrices E_{ij} defined by

$$E_{ij} = \boldsymbol{e}_j^n (\boldsymbol{e}_i^P)^T, \quad i = 1, \dots, P, \quad j = 1, \dots, n.$$

We perform a similarity transformation of the matrices in (3.10) by left-multiplying by E. Note that the the inverse of E is its transpose, E^T. Setting $\boldsymbol{v} = (\boldsymbol{v}_1, \dots, \boldsymbol{v}_P)^T = E\boldsymbol{y}$, we obtain P decoupled eigenvalue problems, each of size $n \times n$,

$$\lambda_i(\boldsymbol{\mu})\boldsymbol{v}_i - D_i(\mathbf{A})\boldsymbol{v}_i, \quad i = 1, \dots, P, \tag{3.11}$$

where $[D_i(\mathbf{A})]_{j,k} = \lambda_i(\boldsymbol{a}_{j,k})$. Assuming that degeneracy due to crossing eigenvalues does not occur, and that there are n distinct eigenvalues of each instance of Eq. (3.11), the gCE coefficients $\boldsymbol{\mu}$ can be obtained from the eigenvalues λ.

Proposition 2. *Assume a multi-dimensional set of P basis functions created by tensor products of one-dimensional basis functions. If each stochastic Galerkin matrix of one-dimensional basis functions is diagonalizable, then the solution of the multi-dimensional MEP is given by P independent standard eigenvalue problems.*

Proof. Let the ordering of the basis functions be lexicographic such that the innermost loop is the first dimension, followed by the second dimension, and so on. By Proposition 2 in Ernst & Ullmann (2010), the multi-dimensional tensor product stochastic Galerkin matrix is given by $G^{\mathrm{SG}} = G_d^{\mathrm{SG}} \otimes G_{d-1}^{\mathrm{SG}} \otimes \cdots \otimes G_1^{\mathrm{SG}}$, where G_k^{SG} $(k = 1, ..., d)$ denotes the one-dimensional stochastic Galerkin matrix of the kth dimension only. Thus, if each one-dimensional eigenvalue decomposition is given by $G_k^{\mathrm{SG}}(\cdot) = Q_k \Lambda_k(\cdot) Q_k^T$, then

$$G^{\mathrm{SG}} = (Q_d \otimes \cdots \otimes Q_1)\,(\Lambda_d \otimes \cdots \otimes \Lambda_1)\,(Q_d \otimes \cdots \otimes Q_1)^T$$

is also an eigenvalue decomposition. The conclusion then follows from Proposition 1.

4. Numerical results

We consider a turbulent premixed combustor composed of a plenum, a burner, a swirled premixed flame and a combustion chamber, as illustrated in Figure 2. This system, known as BRS combustor, has been widely used for the study of combustion noise and combustion instabilities (Komarek & Polifke 2010; Silva *et al.* 2017*b*; Albayrak *et al.* 2017). In this work, each element (plenum, burner, flame, combustion chamber) is represented by a state-space system of equations (Schuermans *et al.* 2002; Emmert *et al.* 2016). We study two different cases. The first one, called combustion noise, consists of assessing the amplitude of the acoustic fluctuations produced by an enclosed source of combustion noise. The second one, termed combustion instability, focuses on the evaluation of the growth

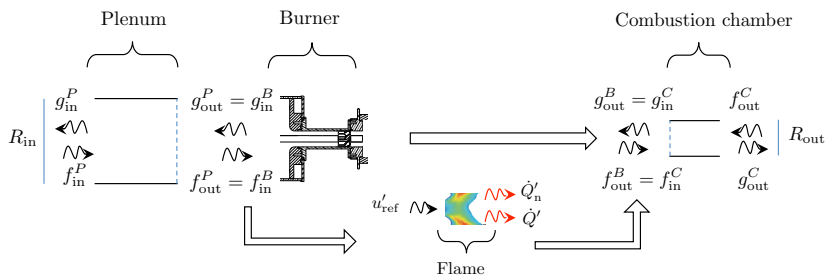

FIGURE 2. Combustor representation with a wave approach.

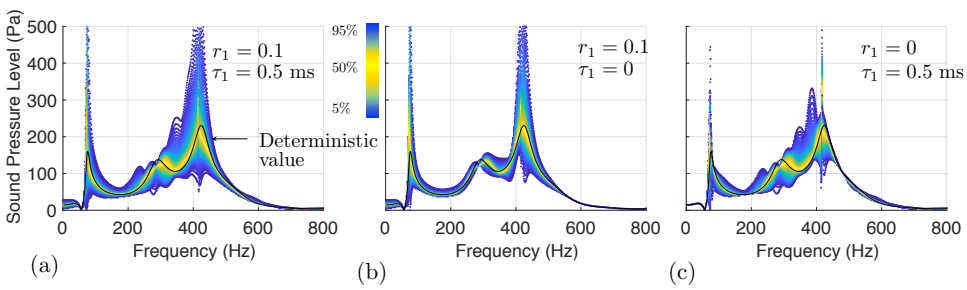

FIGURE 3. Percentiles and deterministic value of combustion noise using iCE with $P = 20$.

rate of the less damped thermoacoustic modes. We consider Ψ_m to be Hermite polynomials and multi-wavelets, respectively. The geometric and thermodynamic parameters considered are the same as in Silva *et al.* (2017*b*).

4.1. *Combustion noise*

We assume uncertainty in the acoustic reflection coefficient at the outlet boundary, given by $r_{\text{out}} = -0.65\Psi_1 + 0.1\Psi_2$, and in the time delay of the acoustic flame response, given by $\tau = (5.0\Psi_1 + 0.5\Psi_2) \cdot 10^{-3}$. Replacing the expansion of r_{out} into the F matrix results in $F = \Psi_1 F_1 + \Psi_2 F_2$. Similarly, the expansion of $1/\tau$ is introduced into matrices $\tilde{A}$ and $\tilde{B}$. The source of combustion noise $\dot{Q}'_{\text{n}}$ is frequency dependent and based on the work of Silva *et al.* (2017*b*). The input of the subsystem 'Burner' is, consequently, given by $\boldsymbol{u} = [f^B_{\text{in}}, g^B_{\text{out}}, \dot{Q}' + \dot{Q}'_{\text{n}}]^\intercal$ (see Figure 2). After building each term $M_{j,k}$ defined by Eq. (3.6), the linear system of Eq. (3.5) is solved for a given value of frequency $s = i\omega$.

Figure 3(a) shows the Sound Pressure Level (SPL) for a range of frequencies between 0 and 800 Hz. The black line illustrates the solution of the deterministic system $(M_{1,1})\boldsymbol{x}_1 = \boldsymbol{b}_1$. Two peaks are observed: a large and broad one at 430 Hz and a smaller one at 80 Hz. From the study of Silva *et al.* (2017*b*), we know that these peaks are associated with a quarter wave mode of the combustion chamber and an Intrinsic ThermoAcoustic (ITA) mode, respectively. Figure 3(a) also shows 100 colored dots per frequency. These dots denote the percentiles of the corresponding PDF: percentiles reaching 50% are yellow, whereas extreme percentiles (approaching 1 or 99%) are blue. The PDF for two different values of frequency is displayed in Figure 4(a,b). Very good agreement is obtained when comparing the results against Monte Carlo simulations with 100,000 samples of Eq. (2.5) for each frequency. Even cases where the PDFs are very skewed or bimodal are well recovered.

In many situations it is important to understand which uncertain parameter dominates the uncertainty of the output random variable (the acoustic field in our case). By means

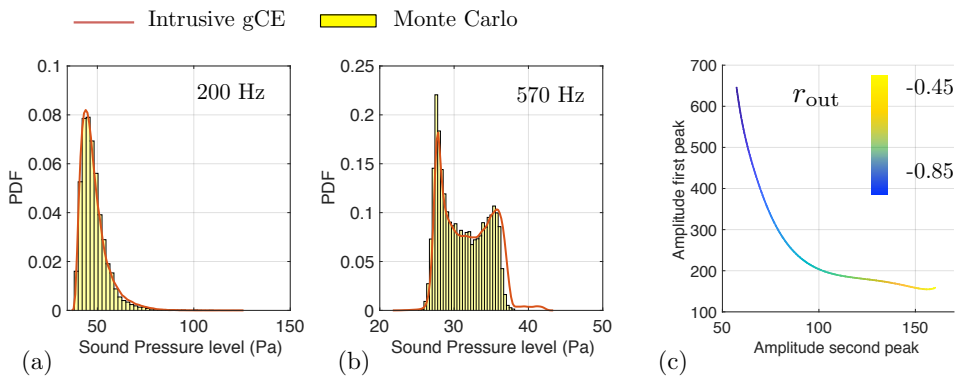

FIGURE 4. (a,b) Probability density function for two frequencies, using Monte Carlo and intrusive Chaos Expansion with $P = 20$. (c) Sensitivity correlation.

of gCE, one can compute the uncertainty at the output, given only one uncertainty at the input, without any additional cost. Using the model obtained for the pressure (given by $\boldsymbol{x} = \sum_{l=1}^{P} \Psi_l \boldsymbol{x}_l$), two SPL (one with $\tau_1 = 0, r_1 = 0.1$ and the other $\tau_1 = 0.5$ ms, $r_1 = 0$) are readily computed. By observing Figure 3 (b,c), we conclude that any uncertainty in r_{out} considerably affects the amplitude of the second peak. The effect of any uncertainty of τ on the peaks amplitude is minor.

An additional question eventually rises: What is the correlation between r_{out} and the amplitude of the first and second peaks? We investigate whether a high value of $r_{\text{out}} > r_0$ or a low value $r_{\text{out}} < r_0$ produces a high amplitude of the first or second peak. Figure 4(c) (right) shows the correlation between the two amplitudes as function of r_{out}. The two peaks are anticorrelated: Whereas a high value of r_{out} induces a high amplitude of the second peak, it induces a low amplitude in the first peak. This type of analysis can be extremely useful when studying combustion noise of enclosed systems, and can be performed at no additional cost.

4.2. *Numerical solution of MEP*

We assume uncertainty in the acoustic reflection coefficient at the outlet boundary, given by $r_{\text{out}} = -0.5 + 0.1\xi_1$, and in the time delay, given by $\tau = 5.5(1 + 0.1\xi_2) \cdot 10^{-3}$, with ξ_1, ξ_2 being uniform random variables on $[-1, 1]$. The basis functions $\{\Psi_m\}$ are multiwavelets, a robust choice due to their hierarchical localization in stochastic space (Le Maître *et al.* 2004). Moreover, the one-dimensional stochastic Galerkin matrix is diagonalizable with constant eigenvectors for zeroth and first-order multiwavelets of all orders, as shown in Pettersson *et al.* (2014). Thus, they satisfy Proposition 1, and a tensor basis of multi-dimensional wavelets satisfies Proposition 2. The method outlined in Section 3.2.1 is used to compute the eigenvalues by solving a sequence of $P = 256$ eigenvalue problems, using a tensor product basis of 16 piecewise linear multiwavelets in each dimension. The most critical eigenvalue in the corresponding deterministic case is the mode with growth rate -28.5 radians per second and frequency 70.3 Hz, and to validate the method we compute its PDF with the proposed method as well as a Monte Carlo reference solution of 100,000 samples, as shown in Figure 5. The PDFs computed from igCE are almost indistinguishable from the reference PDFs. The results show that the critical eigenvalue has a 22% risk of having a positive real part, which means that the system has a 22% risk of being unstable. Both the median and mean values of the real part of the eigenvalue

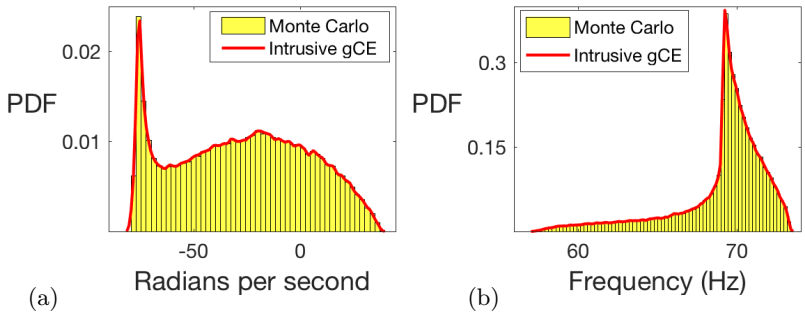

FIGURE 5. Critical eigenvalue $\mu = \sigma + \boldsymbol{i}\omega$, computed with Monte Carlo and intrusive Chaos Expansion with $P = 16 \times 16$ multiwavelets. (a) Probability density function for $\omega/2\pi$. (b) Probability density function for σ.

are slightly positive, despite all eigenvalues of the unperturbed deterministic case having negative real parts.

5. Conclusions

Intrusive generalized chaos expansion has been used for UQ of a generic thermoacoustic state space model with uncertain acoustic boundary conditions and flame response model. The overall methodology is promising for the study of UQ in thermoacoustic systems, since it presents several advantages and novelties:

(*a*) Statistics of interest, including PDFs, can be obtained at a significantly reduced cost compared to Monte Carlo simulation;

(*b*) Although the propagation of input uncertainties to the outputs is highly nonlinear, the igCE method permits the formulation of a very simple system of equations. On the one hand, the system of equations to solve is linear if considering the combustion noise problem. On the other hand, a set of linear decoupled eigenvalue problems result when studying the combustion instability problem;

(*c*) Even though the gCE is applied intrusively to the Stochastic State Space model, the proposed formulation is general and can be applied to different type of models (thermoacoustic networks, acoustic wave equation, linearized Euler equations, etc.);

(*d*) It becomes computationally affordable to perform global sensitivity analysis, defined by methods of variance decomposition, where the influence of inputs on outputs is rigorously evaluated in the entire input space.

REFERENCES

ALBAYRAK, A., STEINBACHER, T., KOMAREK, T. & POLIFKE, W. 2017 Convective Scaling of Intrinsic Thermo-Acoustic Eigenfrequencies of a Premixed Swirl Combustor. *J. Eng. Gas Turbines and Power* **140**, 041510–041510–9.

AVDONIN, A., JAENSCH, S., SILVA, C. F., ČEŠNOVAR, M. & POLIFKE, W. 2018 Uncertainty quantification and sensitivity analysis of thermoacoustic stability with non-intrusive polynomial chaos expansion. *Combust. Flame* **189**, 300–310.

BAUERHEIM, M., NDIAYE, A., CONSTANTINE, P., IACCARINO, G., MOREAU, S. & NICOUD, F. 2014 Uncertainty quantification of thermo-acoustic instabilities in an-

nular combustors. *Proceedings of the Summer Program*, Center for Turbulence Research, Stanford University, pp. 209–218.

Bijl, H., Lucor, D., Mishra, S. & Schwab, C. 2013 *Uncertainty Quantification in Computational Fluid Dynamics*, vol. 92. Springer Science & Business Media.

Browne, P. J. & Sleeman, B. D. 1982 A numerical technique for multiparameter eigenvalue problems. *IMA J. Numer. Anal.* **2**, 451–457.

Emmert, T., Meindl, M., Jaensch, S. & Polifke, W. 2016 Linear state space interconnect modeling of acoustic systems. *Acta Acust. United Ac.* **102**, 824–833.

Ernst, O. & Ullmann, E. 2010 Stochastic Galerkin matrices. *SIAM J. Matrix Anal. A.* **31**, 1848–1872.

Ghanem, R. G. & Spanos, P. D. 1991 *Stochastic Finite Elements: A Spectral Approach*. Courier Corporation.

Komarek, T. & Polifke, W. 2010 Impact of swirl fluctuations on the flame response of a perfectly premixed swirl burner. *J. Eng. Gas Turb. Power* **132**, 061503.

Le Maître, O. & Knio, O. M. 2010 *Spectral Methods for Uncertainty Quantification: With Applications to Computational Fluid Dynamics*. Springer.

Le Maître, O. P., Najm, H. N., Ghanem, R. G. & Knio, O. M. 2004 Multi-resolution analysis of Wiener-type uncertainty propagation schemes. *J. Comput. Phys.* **197**, 502–531.

Lieuwen, T. & Yang, V., ed. 2005 *Combustion Instabilities in Gas Turbine Engines: Operational Experience, Fundamental Mechanisms, and Modeling*, *Progress in Astronautics and Aeronautics*, vol. 210. AIAA.

Magri, L., Bauerheim, M., Nicoud, F. & Juniper, M. P. 2016 Stability analysis of thermo-acoustic nonlinear eigenproblems in annular combustors. Part II. Uncertainty quantification. *J. Comput. Phys.* **325**, 411–421.

Mensah, G. A., Magri, L. & Moeck, J. P. 2018 Methods for the calculation of thermoacoustic stability boundaries and Monte Carlo-free uncertainty quantification. *ASME. J. Eng. Gas Turbines Power* **140**, 061501-061501-10.

Najm, H. N. 2009 Uncertainty quantification and polynomial chaos techniques in computational fluid dynamics. *Annu. Rev. Fluid Mech.* **41**, 35–52.

Nicoud, F., Benoit, L., Sensiau, C. & Poinsot, T. 2007 Acoustic modes in combustors with complex impedances and multidimensional active flames. *AIAA Journal* **45**, 426–441.

Pettersson, P., Iaccarino, G. & Nordström, J. 2014 A stochastic Galerkin method for the Euler equations with Roe variable transformation. *J. Comput. Phys.* **257, Part A**, 481 – 500.

Schuermans, B., Bellucci, V., Nowak, D. & Paschereit, C. O. 2002 Modelling of Complex Thermoacoustic Systems: A State-Space Approach. In *Ninth Int. Congress on Sound and Vibration, ICSV9*. Orlando, FL, USA: IIAV.

Silva, C.F., Magri, L., Runte, T. & Polifke, W. 2017*a* Uncertainty quantification of growth rates of thermoacoustic instability by an adjoint Helmholtz solver. *J. Eng. Gas Turbines and Power* **139**, 011901.

Silva, C. F., Merk, M., Komarek, T. & Polifke, W. 2017*b* The contribution of intrinsic thermoacoustic feedback to combustion noise and resonances of a confined turbulent premixed flame. *Combust. Flame* **182**, 269–278.

Xiu, D. & Karniadakis, G. Em. 2002 The Wiener–Askey polynomial chaos for stochastic differential equations. *SIAM J. Sci. Comput.* **24**, 619–644.